INTERLAMINAR SHEAR STRENGTH AND FAILURE ANALYSIS OF A GLARE LAMINATE

COSTANZO BELLINI , VITTORIO DI COCCO, FRANCESCO IACOVIELLO,
LUCA SORRENTINO

Abstract. Hybrid materials like Fibre Metal Laminates (FMLs) are increasingly valued for their superior mechanical performance, combining high stiffness-to-weight and strength-to-weight ratios with excellent toughness, fatigue resistance, and damage tolerance. This study investigates the interlaminar shear behaviour of a GLARE (Glass Laminate Aluminium Reinforced Epoxy) composite. Mechanical performance was evaluated using a three-point bending test on a short beam to induce a shear stress state. Analysis of the shear stress-displacement curve revealed continuous non-linearity from an early stage, indicating progressive internal damage accumulation. A sudden, catastrophic drop in shear stress immediately after reaching the peak stress suggested interlaminar shear failure. Micrographic analysis confirmed multiple delamination instances within the GLARE specimen.

Key words: GLARE, hybrid composite, interlaminar shear behaviour, damage analysis.

1. INTRODUCTION

Hybrid materials are frequently utilised in various industrial sectors due to their structure, which confers high mechanical performance by combining the characteristics of distinct constituents. Beyond structural applications, the blend of different materials is also suitable for developing novel hybrid materials for non-structural purposes, such as energy applications [1, 2], or simplifying manufacturing processes [3]. Among hybrid materials, Fibre Metal Laminates (FMLs) are increasingly considered for diverse applications [4, 5]. These materials exhibit high stiffness-to-weight and strength-to-weight ratios, attributed to their composite layers, along with good toughness provided by the aluminium sheets [6, 7]. Other notable properties include high fatigue resistance and high damage tolerance, stemming from the composite material component [8, 9].

University of Cassino and Southern Lazio

Ro. J. Techn. Sci. − Appl. Mechanics, Vol. 70, N^{os} 1−3, P. 53−62, Bucharest, 2025

DOI:10.59277/RJTS-AM.2025.1-3.03

FMLs were initially developed for aeronautical applications, leveraging their aforementioned characteristics. The most prevalent type of FML is GLARE (Glass Laminate Aluminium Reinforced Epoxy), which consists of alternating layers of glass fibre-reinforced polymer and aluminium sheets. It is extensively employed in the construction of the Airbus A380, the world's largest aircraft [10]. However, other types of composite materials or metal sheets can be incorporated into the production of such laminates. For instance, carbon fibre-reinforced polymer and aramid fibre-reinforced polymer combined with aluminium foils yield CARALL (Carbon Fibre Reinforced Aluminium Laminate) and ARALL (Aramid Fibre Reinforced Aluminium Laminate), respectively [11, 12]. Similarly, metals other than aluminium can be considered; for example, carbon fibre composite and titanium sheets result in the TiGr (Titanium Graphite) material [13].

Many aircraft components, such as wing leading edges and fuselages, incorporate GLARE. This choice is driven by its excellent combination of damage tolerance, impact, and fatigue resistance, along with its substantial weight-saving potential. GLARE is available in various grades, which are defined by the stacking sequence and fibre orientation of the composite material layers interspersed between the aluminium sheets.

At first glance, one might assume the mechanical characteristics of these laminates are primarily dictated by their constituent materials. However, their ultimate properties depend not only on the starting materials but also crucially on the strength of the interface between the metal sheets and the composite layers. Liu et al. [14] describe a complex system of interfaces within an FML: specifically, the fibre-matrix interface within the composite, the aluminium-composite matrix interface, and the aluminium-fibre interface. This scenario becomes even more intricate if an adhesive layer is introduced into the stacking sequence between the aluminium sheets and the composite material.

Shear stresses from torsion or bending loads can cause the failure of the interface between the hybrid laminate's distinct layers. Indeed, delamination represents the most critical failure mechanism in an FML; the propagation of localised delamination can lead to the failure of the entire structure during service, as described by Pahr et al. [15] and Remmers and De Borst [16]. Consequently, determining the Interlaminar Shear Strength (ILSS) of a laminate is paramount. Numerous tests have been developed and utilised to ascertain this mechanical property. For instance, Hinz et al. [17] conducted a double-notch shear test to calculate laminate ILSS, though this method is susceptible to specimen buckling due to the compressive load applied at its ends. A superior approach for determining laminate ILSS is the three-point bending test on a short beam, a method widely adopted in several research works, including those by Park *et al.* [18] and Bellini *et al.* [6, 8].

The aim of the present article is to analyse the mechanical behaviour of a short beam specimen made of GLARE and subjected to a bending load. In this manner, the ILSS characteristics of the material can be determined. Moreover, the fracture peculiarities were analysed after the mechanical test to better understand the failure mode. The paper is organised in four parts: in the first, the current one, the topic is presented, and a literature survey is reported; in the second, the materials employed in the work and the investigation methods are described. The specimens were tested according to the three-point bending test carried out on a short beam sample. This test setup is simple and effective: by opportunistically setting the span distance between supports, shear stresses become preponderant over normal stresses. The description of the manufacturing process is also reported. The third part describes the results of the study, in terms of loading curves and micrography analysis, while in the last part, conclusions are drawn.

2. MATERIALS AND METHODS

The aim of the present work is to study the mechanical properties of a GLARE laminate, in particular the ILSS, and analyse the fracture mechanisms. Specimens to be tested were extracted from a laminate, produced by prepreg vacuum bagging technology, a widely recognised method for producing high-quality composite parts. As raw material, AA 1100 aluminium sheets, with a thickness of 0.3 mm, and unidirectional glass fibre-epoxy resin prepreg plies, with a thickness of 0.3 mm, were considered. Moreover, a film adhesive, the AF 163 2K, was interposed between the aluminium sheets and the composite material to promote a good adhesion between layers of different materials.

Initially, all necessary components were precisely prepared. This involved cutting three aluminium sheets, twelve glass fibre prepreg plies, and four adhesive patches to the exact dimensions required for the subsequent stacking operation. Following preparation, the layers were arranged in a specific sequence to form the laminate stack: first of all, a metal sheet was placed on the mould and a layer of adhesive was positioned onto it. Then, six prepreg plies were carefully stacked onto this adhesive layer, utilising a cross-ply stratification sequence $[0\text{-}90]_3$ to optimise mechanical properties, as visible in Fig. 1a. After, another ply of adhesive was laid directly on top of the last glass prepreg, as reported in Fig. 1b, and it was followed by the second aluminium sheet, in Fig. 1c. On this second aluminium sheet, the second composite material layer was assembled, consisting of the remaining six prepreg plies along with their necessary two adhesive layers. The stacking sequence was concluded with the placement of the final aluminium sheet on top. Upon completion of the stacking sequence, the assembled laminate was carefully covered with a breather cloth. This crucial layer serves to absorb and collect any excess resin that might be squeezed out during the vacuum and curing processes, ensuring a consistent resin content throughout the laminate. Moreover, it is necessary to guarantee the correct removal of the air during the vacuum operation and gases that are produced by the polymerisation reaction. The entire stack, now covered with the breather cloth, was then sealed securely within a vacuum bag. This bag was connected to a vacuum pump, which was used to evacuate all the air present inside the bag. Creating this vacuum is essential as it compacts the plies, removes trapped air, and helps in consolidating the laminate, preventing voids and improving bond quality. Finally, the mould, sealed within the vacuum bag and with the air evacuated, was transferred into an oven for the cure cycle. During this cycle, controlled heat and time are applied to initiate and complete the polymerisation of the resin, transforming the pliable prepreg layers into a rigid, high-performance composite laminate. The temperature cycle consisted of a first dwell of 30 mins at 77 °C followed by a second dwell at 127 °C for 100 mins.

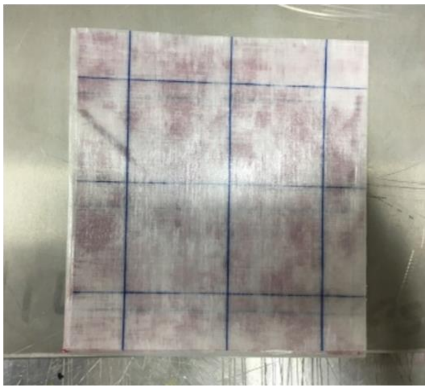

a)

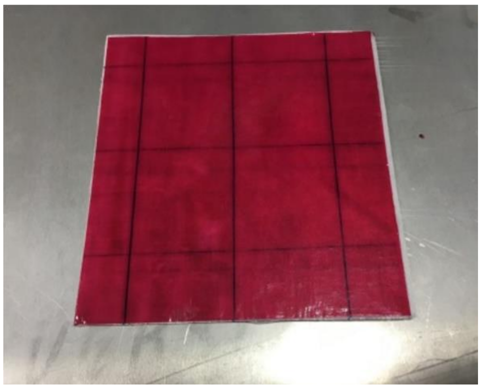

b)

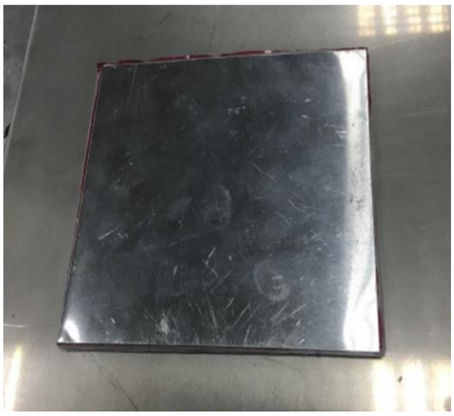

c)

Fig. 1 – Laminate stratification sequence: a) first prepreg stack; b) adhesive layer; c) aluminium sheet.

Following the completion of the cure cycle and the subsequent cool-down in the oven, the produced laminate was extracted from the vacuum bag. To prepare the material for mechanical testing, the laminate was then precisely cut into individual specimens using a diamond disk saw. The specific dimensions of each test specimen were directly determined by the laminate's thickness, according to the ASTM D2344 standard. Given that the laminate thickness measured 5.5 mm, each specimen was cut to a length of 33 mm and a width of 11 mm. This precise sizing is crucial for ensuring consistency and comparability in testing results. Five specimens were prepared and tested for this work.

As previously mentioned, the material's mechanical performance was assessed using the three-point bending test on a short beam. For the purpose of this specific work, certain test parameters were adopted: a span length of 22 mm was set for the testing apparatus, and the loading nose speed was controlled at a constant rate of 1 mm/min. This controlled loading rate ensured accurate measurement of the material response under bending stress, while the reduced span distance allowed for shear stress rise. Figure 2 provides a visual representation of a typical specimen undergoing the three-point bending load, illustrating the setup and application of force during the test.

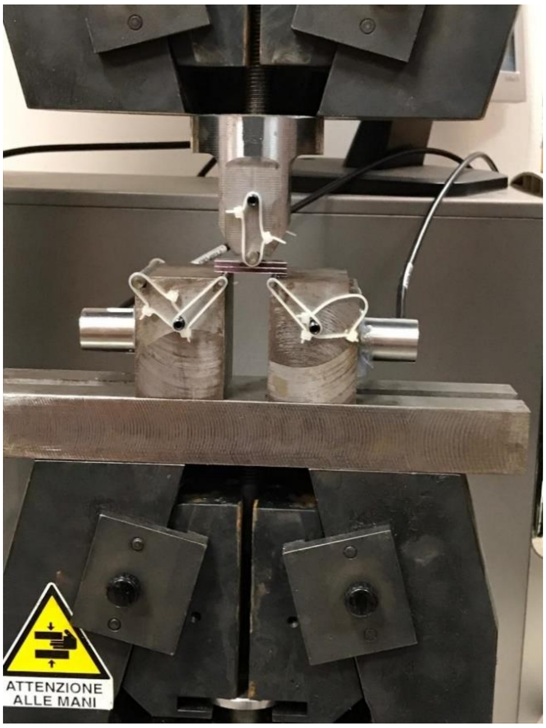

Fig. 2 – Specimen during the three-point bending test.

3. RESULTS

In the present section, the results coming from the experimental test are presented and commented. Figure 3 reports the shear stress trend as a function of the loading displacement. Shear stress τ was calculated from the specimen width b and thickness *h*, and applied load *P* according to Eq. 1:

$$\tau = \left(\frac{3P}{4bh} \right). \tag{1}$$

It is worth noting that, to avoid graph overcrowding, the stress-displacement curve of a single specimen was reported. This was possible since the experimental variance was very low, less than 5%. The initial part of the curve, till 0.17 mm, can be attributed to the seating of the specimen between the supports and the loading nose, and any other minor compliance in the test setup. Beyond this initial settlement, the curve transitions into a region where the material begins to bear the load, but a clear and distinct linear elastic zone followed by a sharp elastic-plastic transition point, as typically observed in ductile metals, is not discernible.

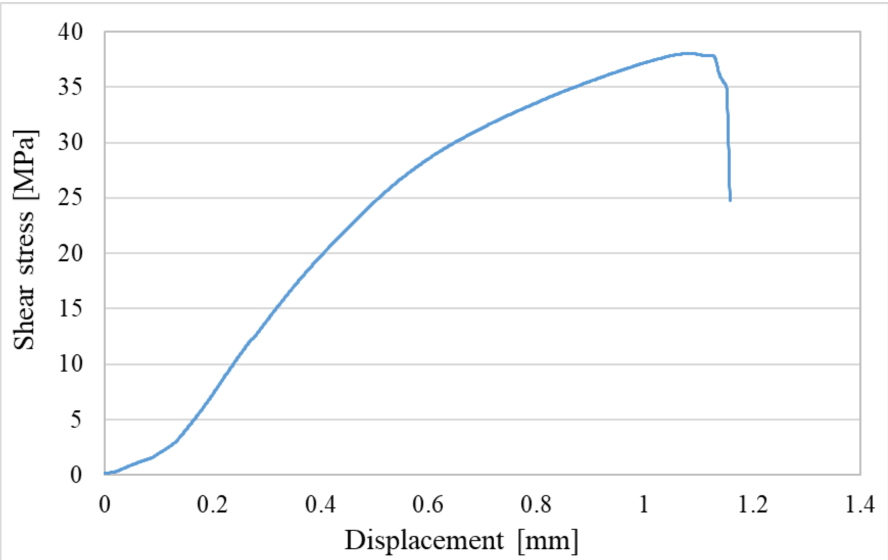

Fig. 3 – Shear stress recorded for the specimen as a function of the displacement.

The continuous non-linearity, without a clear elastic-plastic transition, indicated that damage accumulation is likely occurring progressively within the material from an early stage. This could involve a combination of mechanisms such as matrix micro-cracking, that consist in small cracks forming within the polymer matrix, fibre-matrix debonding, involving the separation of the fibres from the surrounding matrix, and interlaminar damage initiation, that are the early stages of delamination or shear failure at the interfaces between plies. The material continued to absorb energy and carry increasing load, but its effective stiffness was continuously decreasing as internal damage developed. The curve reached its peak shear stress of approximately 39 MPa at a displacement of around 1.1 mm. This represented the ILSS of the material under these test conditions, signifying the maximum load the composite structure could withstand before macroscopic failure. Immediately after reaching the peak stress, there was an abrupt and sharp drop in shear stress. This precipitous fall indicated a sudden, catastrophic failure event within the specimen. Given the nature of the short beam shear test, this was highly indicative of interlaminar shear failure or delamination, where a crack propagated rapidly along the interfaces between the composite layers. The steepness of this drop signified a brittle or quasi-brittle failure mode in terms of interlaminar shear.

To better understand and determine the failure mode, the micrographic analysis of the specimens was carried out. The lateral surface of the specimens, that is the surface parallel to the load direction, was observed through a Leica VM2000 digital microscope. The analysis of the micrographs revealed different instances of delamination within the GLARE specimen following load application. A significant failure occurred near the interface between the top aluminium layer, where the load was applied, and the first composite ply, whose fibres are oriented in the longitudinal direction of the specimen. As visible in Fig. 4, the first composite layer resulted delaminated.

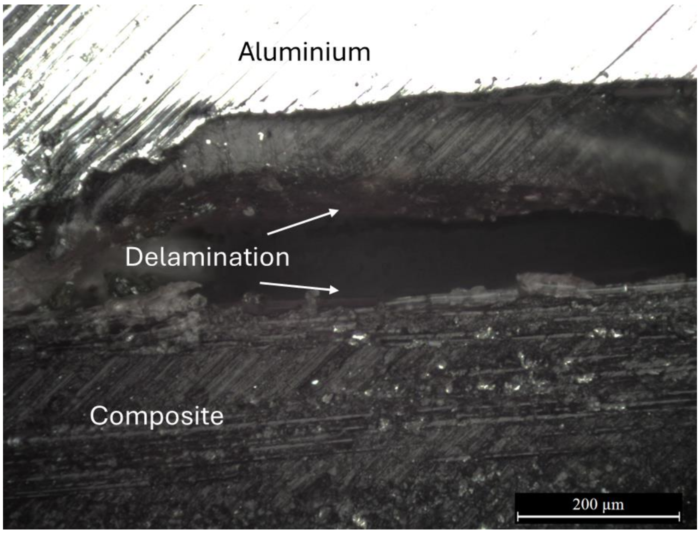

Fig. 4 – Delamination of the first composite layer, near the interface with the top aluminium sheet.

Further damage was evident in the central region of the laminate thickness, as witnessed by Fig. 5. Here, delamination was observed between the fourth and fifth composite plies, where the former was characterised by fibres oriented at 90° with respect to the specimen longitudinal axis. This failure manifested as extensive interfacial debonding between these two layers. Then, the crack propagated from this interface into the interior of the fourth composite ply. This path of crack propagation occurred in a region where the 90° oriented fibres offered minimal resistance to fracture. The crack likely travelled among the fibres in that 90-degree layer, a much easier path than trying to break through the strong fibres themselves.

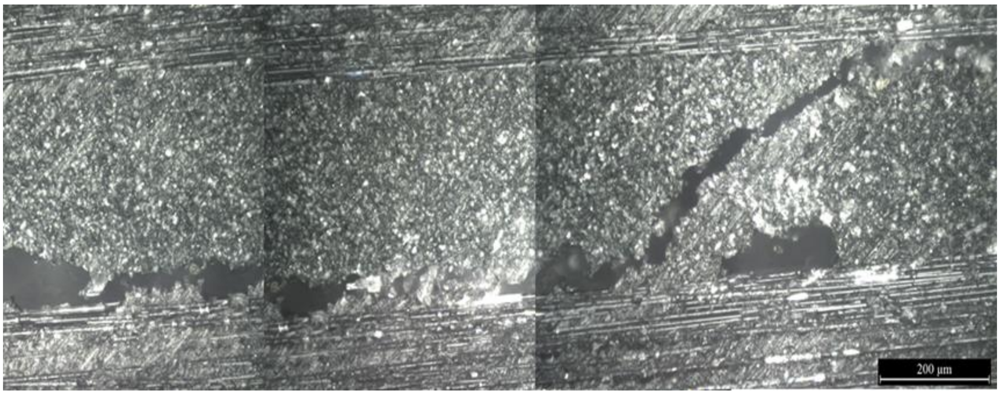

Fig. 5 – Delamination between fourth and fifth composite plies.

4. CONCLUSIONS

In the present work, the interlaminar shear behaviour of a GLARE (Glass Laminate Aluminium Reinforced Epoxy) has been studied, and the morphology of the broken specimen was analysed to determine the damage mode. The mechanical performances of the manufactured specimens were evaluated through the three-point bending test on a short beam: in this manner, a shear stress state was induced in the laminate.

Analysing the shear stress-displacement curve, it was found that the material exhibited continuous non-linearity from an early stage, suggesting that internal damage accumulated progressively. Immediately after reaching the peak stress, there was an abrupt and sharp drop in shear stress, indicative of a sudden, catastrophic failure event, suggesting interlaminar shear failure.

The micrographic analysis revealed multiple instances of delamination within the GLARE specimen after load application. A significant failure was observed in the first composite ply, near the top aluminium sheet. Further damage was evident in the central region of the laminate thickness, between the fourth and fifth composite plies. This failure manifested as extensive interfacial debonding between these two layers, that propagated from this interface into the interior of the fourth composite ply, where the 90°-oriented fibres offered minimal resistance to fracture.

Received on June 28, 2025

REFERENCES

1. MISTEWICZ, K., JESIONEK, M., NOWAK, M., KOZIOL, M., *SbSeI pyroelectric nanogenerator for a low temperature waste heat recovery*, Nano Energy, **64**, article 103906, 2019.
2. TOROŃ, B., SZPERLICH, P., KOZIOL, M., *SbSI Composites based on epoxy resin and cellulose for energy harvesting and sensors-the influence of SBSI nanowires conglomeration on piezoelectric properties*, Materials, **13**, pp. 902–915, 2020.
3. DING, Z., WANG, H., LUO, J., LI, N., *A review on forming technologies of fibre metal laminates*, Int. J. Lightweight Mater. Manuf., **4**, pp. 110–126, 2021.
4. OSTAPIUK, M., BIENIAŚ, J., SUROWSKA, B., *Analysis of the bending and failure of fiber metal laminates based on glass and carbon fibers*, Sci. Eng. Compos. Mater., **25**, pp. 1095–1106, 2017.
5. AHMADI, H., SABOURI, H., LIAGHAT, G., BIDKHORI, E., *Experimental and numerical investigation on the high velocity impact response of GLARE with different thickness ratio*, Procedia Eng., **10**, pp. 869–874, 2011.
6. BELLINI, C., DI COCCO V., SORRENTINO, L., *Interlaminar shear strength study on CFRP/Al hybrid laminates with different properties*, Fract. Struct. Integr., **51**, pp. 442–448, 2020.
7. VERMEEREN, C.A.J.R., *An Historic Overview of the Development of Fibre Metal Laminates*, Appl. Compos. Mater., **10**, pp. 189–205, 2003.
8. TANG, D., HUANG, H., FAN, Y., WANG, H., PENG, Y., *Manufacturing and impact resistance of Large-Scale stacked fibre metal laminates*, Mater. Des., **253** (article 113917), 2025.
9. BELLINI, C., DI COCCO V., IACOVIELLO, F., SORRENTINO, L., *Failure energy and strength of Al/CFRP hybrid laminates under flexural load*, Mater. Des. Process. Commun., pp. 1–6, 2019.
10. LI, H., HU, Y., XU, Y., ZHENG, X., LIU, H., TAO, J., *Reinforcement effects of aluminumelithium alloy on the mechanical properties of novel fiber metal laminate*, Compos. Part B Eng., **82**, pp. 72–77, 2015.
11. BELLINI, C., DI COCCO V., IACOVIELLO, F., SORRENTINO, L., *Flexural strength of aluminium carbon/epoxy fibre metal laminates*, Mater. Des. Process. Commun., **1**, p. e40, 2019.
12. BELLINI, C., DI COCCO V., IACOVIELLO, F., SORRENTINO, L., *Performance evaluation of CFRP/Al fibre metal laminates with different structural characteristics*, Compos. Struct., **225**, pp. 111117, 2019.
13. LI, X., ZHANG, X., ZHANG, H., YANG, J., NIA A.B., CHAI, G.B., *Mechanical behaviors of Ti/CFRP/Ti laminates with different surface treatments of titanium sheets*, Compos. Struct., **163**, pp. 21–31, 2017.

14. LIU, C., DU, D., LI, H., HU, Y., XU, Y., TIAN J., et al., *Interlaminar failure behavior of GLARE laminates under short-beam three-point-bending load*, Compos. Part B Eng., **97**, pp. 361–367, 2016.
15. PAHR, D.H., RAMMERSTORFER, F.G., ROSENKRANZ, P., HUMER, K., WEBER, H.W., *A study of short-beam-shear and double-lap-shear specimens of glass fabric/epoxy composites*, Compos. Part B Engineering, **33**, pp. 125–132, 2002.
16. REMMERS, J.J.C., DE BORST, R., *Delamination buckling of fibre-metal laminates*, Compos. Sci. Technol., **61**, pp. 2207–2213, 2001.
17. HINZ, S., OMOORI, T., HOJO, M., SCHULTE, K., *Damage characterisation of fibre metal laminates under interlaminar shear load*, Compos. Part A Appl. Sci. Manuf., **40**, pp. 925–931, 2009.
18. PARK, S.Y., CHOI, W.J., CHOI, H.S., KWON, H., *Effects of surface pre-treatment and void content on GLARE laminate process characteristics*, J. Mater. Process. Technol., **210**, pp. 1008–1016, 2010.